

Low-lying Structures Of Exotic Sc Isotopes And The Evolution Of The $N = 34$ Subshell Closure

D. Steppenbeck^{*a}, S. Takeuchi,^b N. Aoi,^c P. Doornenbal,^a M. Matsushita,^d H. Wang,^a
H. Baba,^a S. Go,^d J. Lee,^a K. Matsui,^e S. Michimasa,^d T. Motobayashi,^a
D. Nishimura,^f T. Otsuka,^{d,e} H. Sakurai,^{a,e} Y. Shiga,^g P.-A. Söderström,^a
T. Sumikama,^h R. Taniuchi,^e Y. Utsuno,ⁱ J. J. Valiente-Dobón,^j and K. Yoneda^a

^aRIKEN Nishina Center, 2-1, Hirosawa, Wako, Saitama 351-0198, Japan

^bDepartment of Physics, Tokyo Institute of Technology, Meguro, Tokyo 152-8551, Japan

^cResearch Center for Nuclear Physics, University of Osaka, Ibaraki, Osaka 567-0047, Japan

^dCenter for Nuclear Study, University of Tokyo, Hongo, Bunkyo, Tokyo 113-0033, Japan

^eDepartment of Physics, University of Tokyo, Hongo, Bunkyo, Tokyo 113-0033, Japan

^fDepartment of Physics, Tokyo University of Science, Noda, Chiba 278-8510, Japan

^gDepartment of Physics, Rikkyo University, Toshima, Tokyo 171-8501, Japan

^hDepartment of Physics, Tohoku University, Sendai, Miyagi 980-8578, Japan

ⁱJapan Atomic Energy Agency, Tokai, Ibaraki 319-1195, Japan

^jInstituto Nazionale di Fisica Nucleare, Laboratori Nazionali di Legnaro, Legnaro 35020, Italy

E-mail: steppenbeck@riken.jp

Recent investigations of exotic nuclei with $N = 32$ and 34 have highlighted the presence of sizable subshell closures at these neutron numbers that are absent in stable isotones. Indeed, the development of the shell gap at $N = 32$ is now well established from studies along the calcium, titanium, and chromium isotopic chains and, more recently, below the $Z = 20$ core in potassium and argon isotones. The onset of a new subshell closure at $N = 34$ was reported in ^{54}Ca owing to the relatively high energy of its first 2^+ state. On the theoretical side, the development of these neutron subshell gaps has been discussed, for example, in the framework of tensor-force-driven shell evolution; as protons are removed from the $\pi f_{7/2}$ orbital, the $\nu f_{5/2}$ state becomes progressively less bound and shifts up in energy relative to the $\nu p_{3/2} - \nu p_{1/2}$ spin-orbit partners. However, it was also reported that no significant $N = 34$ subshell gap exists in titanium, despite the fact that an inversion of the $\nu f_{5/2}$ and $\nu p_{1/2}$ orbitals has been noted. Thus, the strength of the $N = 34$ subshell closure in the scandium isotopes, which lie between calcium and titanium, provides additional insight on the migration of the $\nu f_{5/2}$ orbital in exotic nuclei. In the present work, the low-lying structures of the neutron-rich isotopes ^{54}Sc , ^{55}Sc , and ^{56}Sc —investigated using in-beam γ -ray spectroscopy with fast radioactive projectiles—will be presented, and the evolution of the $N = 34$ subshell closure will be further examined. The results will be compared to modern shell-model calculations applied within the pf shell.

*The 26th International Nuclear Physics Conference
11-16 September, 2016
Adelaide, Australia.*

*Speaker.

1. Introduction

The neutron-rich fp shell is bounded by the proton and neutron numbers $Z = 20$ –28 and $N = 28$ –40. For exotic nuclei in this mass region, an attractive nucleon-nucleon interaction between the $\pi f_{7/2}$ and $\nu f_{5/2}$ proton and neutron orbitals has been discussed, for example, in the framework of tensor-force-driven shell evolution [1], as being responsible for nuclear shell evolution around $Z = 20$. Namely, as protons are removed from the $\pi f_{7/2}$ orbital (from Ni to Ca), the strength of the interaction weakens, causing the neutron $\nu f_{5/2}$ state to shift up in energy relative to the $\nu p_{3/2}$ – $\nu p_{3/2}$ spin-orbit partners. This leads to the possible development of new neutron subshell closures at $N = 32$ and 34 in exotic nuclei approaching calcium, as illustrated in Fig. 1 of Ref. [2].

Prior to the experiment of the present work, which is outlined in Section 2, the development of subshell gaps at $N = 32$ was reported in ^{52}Ca [3, 4], ^{54}Ti [5, 6], and ^{56}Cr [7, 8] from systematics of first 2^+ energies [$E(2_1^+)$] and $B(E2)$ transition rates. However, no significant $N = 34$ subshell closure was observed in either ^{56}Ti [6, 9] or ^{58}Cr [7, 8], while input from theoretical calculations in the case of ^{54}Ca was unclear owing to a large divergence of predicted $E(2_1^+)$ values for this isotope. It is also noted that, more recently, the $N = 32$ subshell closure was confirmed in Ca isotopes from high-precision mass measurements using the multi-reflection time-of-flight method [10], and experimental evidence has emerged for the persistence of the $N = 32$ gap in nuclei ‘south’ of the $Z = 20$ shell, namely, in K [11] and Ar [12] isotones. Interestingly, however, the double magicity of ^{52}Ca has been questioned based on measurements of nuclear charge radii deduced from laser spectroscopy experiments [13]. In order to clarify the strength of the $N = 34$ subshell closure in nuclei further from stability, the structures of the exotic isotones ^{54}Ca and ^{55}Sc were investigated in the present work. New results on the neighbouring isotopes ^{54}Sc and ^{56}Sc are also presented.

2. Experiment

The nuclei of interest—exotic $N \sim 34$ isotopes around $Z = 20$ —were studied using the technique of in-beam γ -ray spectroscopy at the RIKEN Radioactive Isotope Beam Factory (RIBF); a schematic layout of the facility is provided in Fig. 1.

Projectile fragmentation of a primary beam of $^{70}\text{Zn}^{30+}$ ions at 345 MeV/u was adopted to create very neutron-rich $N = 34$ isotones; the BigRIPS separator [14] was employed to create a secondary beam that was optimized for the transmission of ^{55}Sc . It is noted that ^{56}Ti also fell within the acceptance of the spectrometer. The secondary beam was focused on a 10-mm-thick Be reaction target located at the F8 focal plane, and reaction products were identified by the ZeroDegree spectrometer [14] operating in the large-acceptance mode and tuned for the transmission of ^{54}Ca . Examples of particle identification plots for BigRIPS and ZeroDegree are available in Refs. [2], [12], and [15]. The Be target was placed within the DALI2 γ -ray detector array [16], which consisted of 186 large-volume NaI(Tl) detectors, to measure γ radiation emitted from nuclear excited states populated by the reactions. The typical primary beam intensity was ~ 60 pA, and the rates of ^{55}Sc and ^{56}Ti delivered to the F8 target area were ~ 12 and 125 particles per second per pA of primary beam, respectively. Data acquisition was triggered by the arrival of an ion at the F11 focal plane in coincidence with at least one γ ray in DALI2; data were collected in this way for a total of approximately 40 hours.

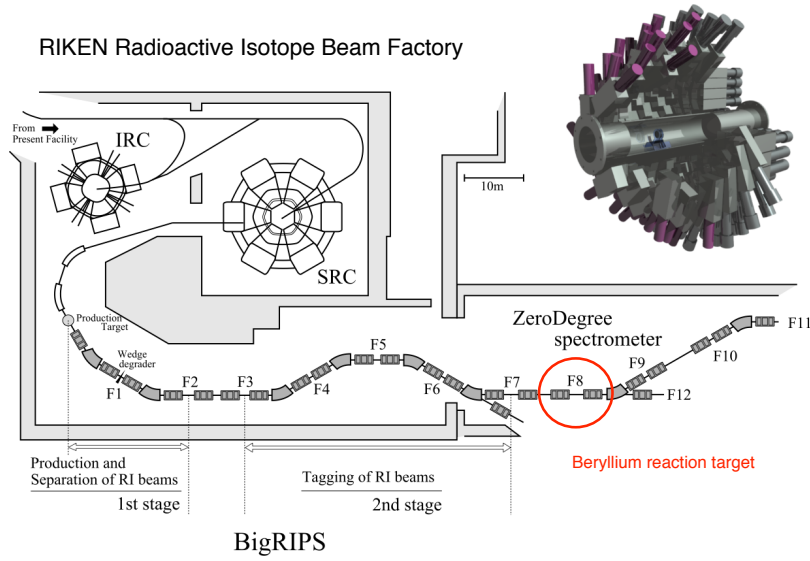


Figure 1: Schematic layout of the RIKEN RIBF facility. The DALI2 γ -ray detector array, which was located at the F8 target position throughout the experiment, is displayed in the top right-hand corner.

3. Results and discussion

3.1 In-beam γ -ray spectroscopy of ^{54}Ca

Excited states in ^{54}Ca were measured for the first time using $\text{Be}(^{55}\text{Sc}, ^{54}\text{Ca}+\gamma)$ and $\text{Be}(^{56}\text{Ti}, ^{54}\text{Ca}+\gamma)$ proton-removal reactions. The Doppler-corrected γ -ray energy spectrum, which is displayed in Fig. 4(a) of Ref. [2], indicates that the 2_1^+ state in ^{54}Ca lies at an energy of 2,043 keV, which is lower, but comparable to the value in ^{52}Ca [3, 4]. Given the fact that $E(2_1^+)$ for ^{54}Ca is enhanced relative to other Ca isotopes, such as ^{50}Ca , as well as $E(2_1^+)$ values in other $N = 34$ isotones, a new subshell closure in ^{54}Ca is proposed. In order to make a more quantitative statement on the matter, large-scale shell-model calculations were performed using the GXPFI1Br effective interaction [2]. The calculations indicate that, firstly, the 2_1^+ state in ^{54}Ca can be understood primarily as a neutron particle-hole excitation across the $N = 34$ subshell closure ($\nu f_{5/2} \otimes \nu p_{1/2}^{-1}$), and, secondly, the magnitude of the $N = 34$ subshell closure in calcium isotopes ($\nu p_{1/2} - \nu f_{5/2}$ effective single-particle energy gap) is similar to that of the $N = 32$ subshell gap ($\nu p_{3/2} - \nu p_{1/2}$ effective single-particle energy gap). In fact, despite the lower $E(2_1^+)$ value in ^{54}Ca relative to ^{52}Ca , the calculations suggest that both subshell closures are ~ 2.5 MeV in magnitude.

3.2 In-beam γ -ray spectroscopy of ^{54}Sc , ^{55}Sc , and ^{56}Sc

Thus, a sizable subshell closure exists in ^{54}Ca that disappears with two protons occupying the $\pi f_{7/2}$ orbital (Ti isotopes); it is, therefore, natural to investigate the situation intermediate to these cases—the Sc isotopes—which contain only one proton in the $\pi f_{7/2}$ orbital. This provides further insight on the evolution of the neutron $\nu f_{5/2}$ state in exotic nuclei.

The γ -ray energy spectra for ^{55}Sc deduced in the present work for the $^9\text{Be}(^{55}\text{Sc}, ^{55}\text{Sc}+\gamma)$ and $^9\text{Be}(^{56}\text{Ti}, ^{55}\text{Sc}+\gamma)$ reactions are presented in Figs. 2(a) and 2(b), respectively. No results on excited states in ^{55}Sc were reported prior to the present experiment. In the case of the inelastic scattering

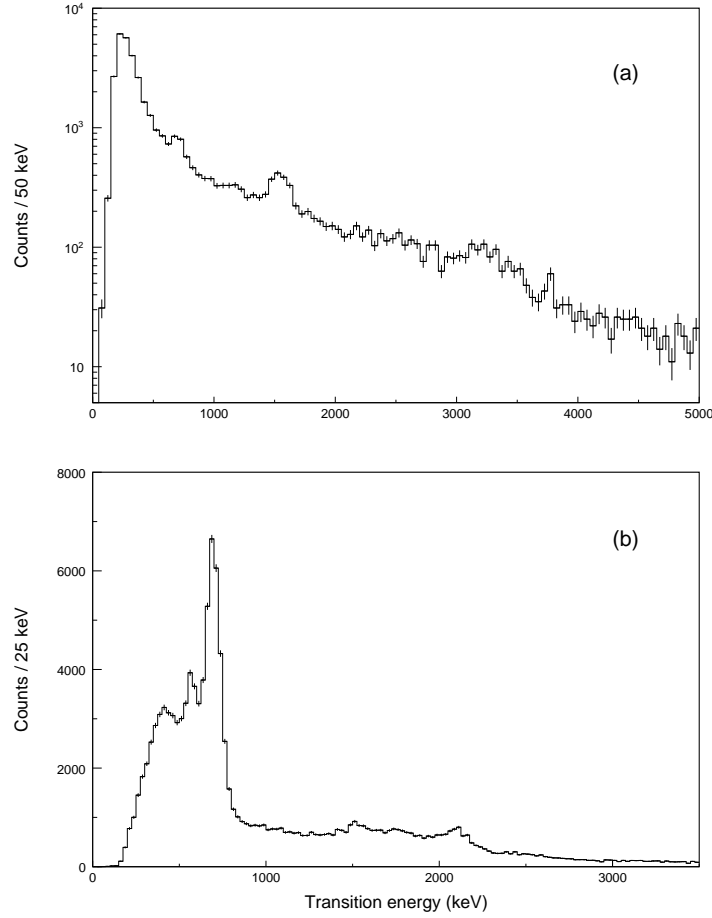


Figure 2: Doppler-corrected γ -ray energy spectra for the (a) ${}^9\text{Be}({}^{55}\text{Sc}, {}^{55}\text{Sc}+\gamma)$ inelastic scattering and (b) ${}^9\text{Be}({}^{56}\text{Ti}, {}^{55}\text{Sc}+\gamma)$ one-proton removal reactions deduced in the present work. Results are preliminary.

spectrum of Fig. 2(a), three γ -ray peaks are located at 0.71(1), 1.54(2), and 3.24(4) MeV. However, a larger number of peaks are present in the one-proton removal reaction of Fig. 2(b), which contains a multiplet of at least five transitions within the energy range ~ 1.5 – 2.5 MeV, and an additional peak at 0.58(1) MeV. (Note, however, that the peak at 3.24(4) MeV in Fig. 2(a) is not observed in the one-proton removal spectrum.) Because the relative intensity of the 0.7-MeV line in Fig. 2(b) is significantly larger than any of the other transitions in the spectrum, it is likely that this γ ray depopulates a state at 0.7 MeV and feeds the ground state directly; however, this proposed decay scheme requires confirmation from $\gamma\gamma$ coincidence relationships in the future. By comparing the suggested energy of this experimental level to predictions of the GXPF1Br effective interaction, it is proposed that the 0.7-MeV level is the counterpart of the $3/2^-$ shell-model state, which lies at ~ 600 keV. In the case of ${}^{53}\text{Sc}$, it was reported that the first $3/2^-$ level is part of a multiplet of states that result from a $\pi f_{7/2} \otimes {}^{52}\text{Ca}(2_1^+)$ configuration [17]. While the multiplet of levels in ${}^{53}\text{Sc}$ lies at an energy comparable to $E(2_1^+)$ in ${}^{52}\text{Ca}$, indicating a rather robust $N = 32$ subshell closure, the energy of the proposed first $3/2^-$ level in ${}^{55}\text{Sc}$ is significantly lower than the yrast 2^+ state in ${}^{54}\text{Ca}$ [2]. This suggests a rather rapid weakening of the $N = 34$ subshell closure, even with only

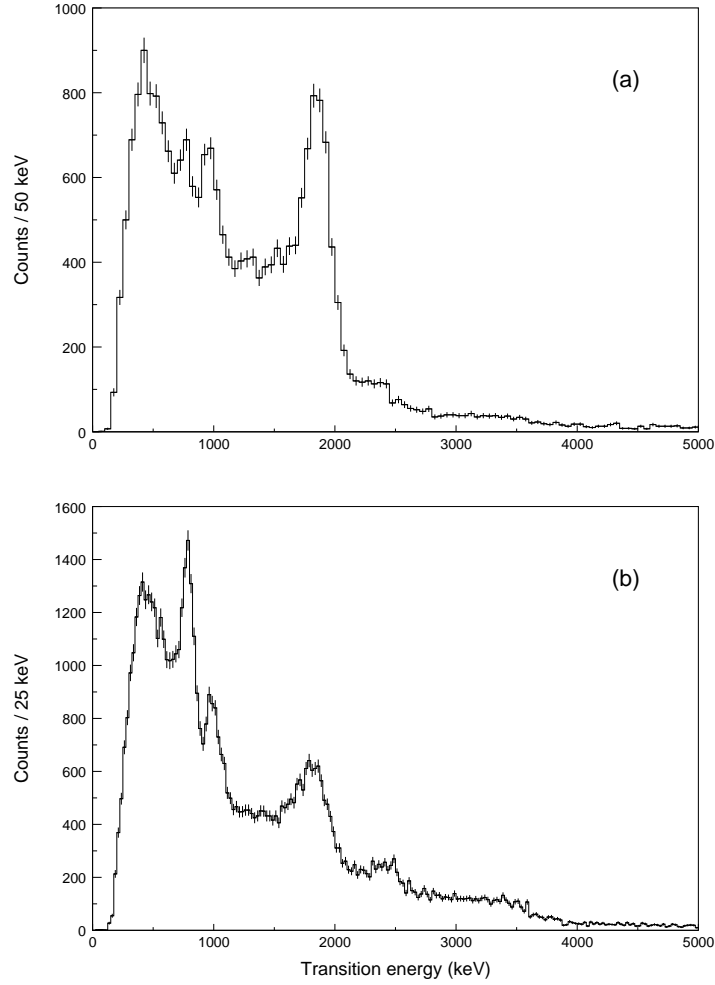


Figure 3: Doppler-corrected γ -ray energy spectra for the (a) ${}^9\text{Be}({}^{55}\text{Sc}, {}^{54}\text{Sc}+\gamma)$ one-neutron removal and (b) ${}^9\text{Be}({}^{56}\text{Ti}, {}^{54}\text{Sc}+\gamma)$ proton-neutron removal reactions deduced in the present work. Results are preliminary.

one proton occupying the $\pi f_{7/2}$ orbital.

The structures of ${}^{54}\text{Sc}$ and ${}^{56}\text{Sc}$ were also investigated in the present work using a variety of reactions including nucleon removal and charge exchange. Spectroscopy of ${}^{54}\text{Sc}$ was performed using ${}^9\text{Be}({}^{55}\text{Sc}, {}^{54}\text{Sc}+\gamma)$ one-neutron removal and ${}^9\text{Be}({}^{56}\text{Ti}, {}^{54}\text{Sc}+\gamma)$ proton-neutron removal reactions, which are presented in Figs. 3(a) and 3(b), respectively. Two levels in ${}^{54}\text{Sc}$ were previously identified in decay studies [17, 18, 19]: One $(1)^+$ level at 247 keV, and a $(4, 5^+)$ isomeric state at 110 keV. The present study was not sensitive to these transitions owing to DALI2 detector threshold settings. The two spectra displayed in Fig. 3 contain the same energy transitions as each other, albeit with different relative intensities, up to ~ 2 MeV; however, the spectrum of Fig. 3(b) contains several additional γ -ray peaks up to ~ 3.5 MeV. The ${}^{54}\text{Sc}$ level scheme is currently in progress and is, therefore, not provided here.

In the case of ${}^{56}\text{Sc}$, respective $(2)^+$ and $(3)^+$ levels at 587 and 727 keV were previously reported, in addition to a $(4)^+$ isomeric state ($T_{1/2} = 290 \pm 30$ ns) at 775 keV [17, 18]. A longer-lived, β -decaying isomer ($T_{1/2} = 75 \pm 6$ ms) with spin-parity values of $(5, 6)^+$ [17] also exists in

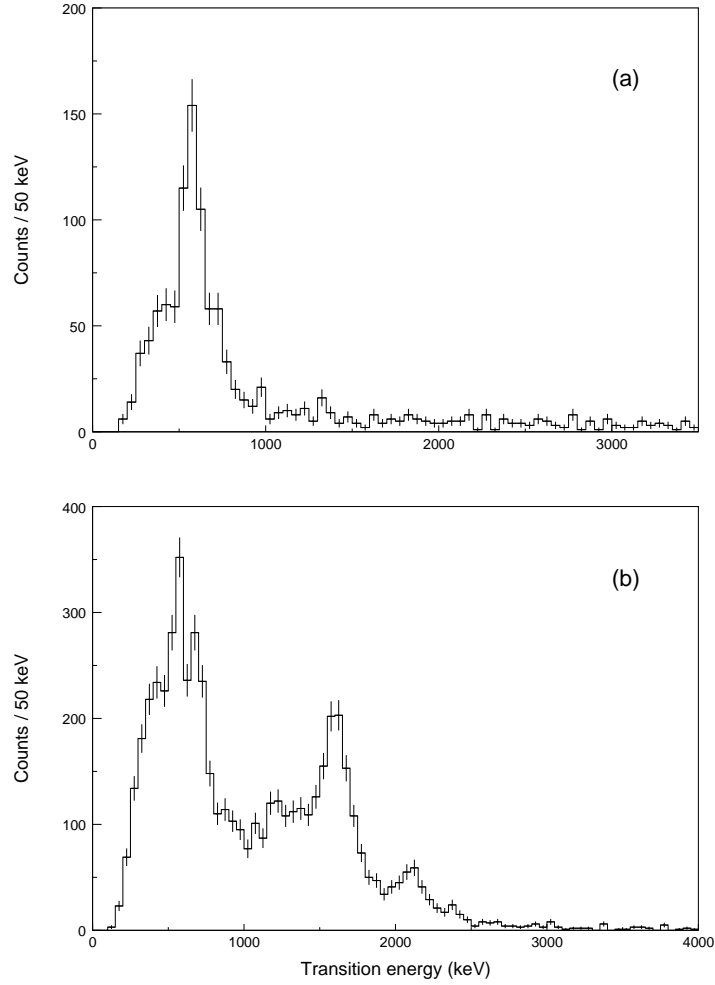


Figure 4: Doppler-corrected γ -ray energy spectra for the (a) ${}^9\text{Be}({}^{57}\text{Ti}, {}^{56}\text{Sc}+\gamma)$ one-proton removal and (b) ${}^9\text{Be}({}^{56}\text{Ti}, {}^{56}\text{Sc}+\gamma)$ charge-exchange reactions deduced in the present work. Results are preliminary.

${}^{56}\text{Sc}$, although the energy of that state is currently unknown. Several low-energy transitions were also reported in Refs. [17, 18], specifically at 48, 140, and 188 keV, although the present experiment was not sensitive to those γ rays owing to DALI2 threshold settings. The structure of ${}^{56}\text{Sc}$ was investigated in the current study using ${}^9\text{Be}({}^{57}\text{Ti}, {}^{56}\text{Sc}+\gamma)$ one-proton removal and ${}^9\text{Be}({}^{56}\text{Ti}, {}^{56}\text{Sc}+\gamma)$ charge-exchange reactions, which are displayed in Figs. 4(a) and 4(b), respectively. The two lowest-energy transitions observed in the two spectra are consistent in energy, and they likely correspond to the γ rays reported at 587 and 727 keV in the earlier decay studies [17, 18]. The multiplet of transitions observed in Fig. 4(b) in the energy range ~ 1.0 – 2.5 MeV, which are not present in the spectrum of Fig. 4(a), must depopulate states at higher energies than those previously reported [17, 18], although the details of the level scheme cannot be provided at the present time.

4. Summary

The structures of ^{54}Sc , ^{55}Sc , and ^{56}Sc were investigated using the technique of in-beam γ -ray spectroscopy with a variety of reactions including nucleon removal, charge exchange, and inelastic scattering at the RIKEN Radioactive Isotope Beam Factory to shed further light on the development of the $N = 34$ subshell closure approaching $Z = 20$. The low-lying structure of the $N = 34$ isotope (^{55}Sc) indicates a probable $3/2_1^-$ state at 0.7 MeV, which lies well below the energy of the first 2^+ level in ^{54}Ca , suggesting a rapid weakening of the $N = 34$ subshell gap even with only one proton occupying the $\pi f_{7/2}$ orbital. This situation differs to that previously reported [17] for ^{53}Sc and ^{52}Ca , where the respective $3/2_1^-$ and 2_1^+ states lie at comparable energies, highlighting the robust nature of the $N = 32$ subshell closure. The γ -ray energy spectra deduced for ^{54}Sc and ^{56}Sc contribute additional information to the structures of these isotopes reported in previous decay studies [17, 18, 19], although the details of the extended level schemes cannot be provided here.

Acknowledgements

We thank the RIKEN Nishina Center accelerator staff and the BigRIPS team for their valuable contributions to the experiment.

References

- [1] T. Otsuka *et al.*, Phys. Rev. Lett. **95** (2005) 232502.
- [2] D. Steppenbeck *et al.*, Nature (London) **502** (2013) 207–210.
- [3] A. Huck *et al.*, Phys. Rev. C **31** (1985) 2226–2237.
- [4] A. Gade *et al.*, Phys. Rev. C **74** (2006) 021302(R).
- [5] R. V. F. Janssens *et al.*, Phys. Lett. B **546** (2002) 55–62.
- [6] D.-C. Dinca *et al.*, Phys. Rev. C **71** (2005) 041302(R).
- [7] J. I. Prisciandaro *et al.*, Phys. Lett. B **510** (2001) 17–23.
- [8] A. Bürger *et al.*, Phys. Lett. B **622** (2005) 29–34.
- [9] S. N. Liddick *et al.*, Phys. Rev. Lett. **92** (2004) 072502.
- [10] F. Wienholtz *et al.*, Nature (London) **498** (2013) 346–349.
- [11] M. Rosenbusch *et al.*, Phys. Rev. Lett. **114** (2015) 202501.
- [12] D. Steppenbeck *et al.*, Phys. Rev. Lett. **114** (2015) 252501.
- [13] R. F. Garcia Ruiz *et al.*, Nature Physics **12** (2016) 594–598.
- [14] T. Kubo *et al.*, Prog. Theor. Exp. Phys. **2012** (2012) 03C003.
- [15] D. Steppenbeck *et al.*, JPS Conf. Proc. **6** (2015) 020019.
- [16] S. Takeuchi *et al.*, Nucl. Instrum. Methods Phys. Res. A **763** (2014) 596–603.
- [17] H. L. Crawford *et al.*, Phys. Rev. C **82** (2010) 014311.
- [18] S. N. Liddick *et al.*, Phys. Rev. C **70** (2004) 064303.
- [19] P. F. Mantica *et al.*, Phys. Rev. C **77** (2008) 014313.